CUSTOMER **CONTRACT OFFICER** **TECHNICAL OFFICER**	**ESA/ESTEC** **Christophe Seynaeve** **Maria Nestoridi**
CONTRACT TITLE	**Innovative High Energy Density Li-ion batteries operating at low temperature /HELT-Bat**
CONTRACT NUMBER	**4000123741/18/NL/CRS**
CONTRACTOR	**DUTH**
SUBCONTRACTORS	**CERTH** **AIRBUS DS**
DELIVERABLE	**ESR**
TITLE	**Executive Summary Report**
DELIVERY DATE	**30-11-2020**
DUE DATE	**30-11-2020**

Innovative High Energy Density Li-ion batteries operating at low temperature /HELT-Bat

Executive Summary Report

F. FARMAKIS(1), S. THIRUVENGADAM(1), C. ELMASIDES(1)
D. TSIPLAKIDES(2), S. BALOMENOU(2), N. STRATAKI(2)
M. CARRERAS(3), O. GUINARD(3), W. BREVET(3), B. SAMANIEGO(3)
farmakis@ee.duth.gr, dtsiplak@certh.gr, bruno.samaniego@airbus.com

(1) Democritus University of Thrace (DUTH), Xanthi, Greece
(2) Centre for Research and Technology-Hellas (CERTH), Thessaloniki, Greece
(3) Airbus Defence and Space (AIRBUS DS), Toulouse, France

ESA CONTRACT Nº 4000123741/18/NL/CRS
ESA Technical Officer: Maria NESTORIDI
Maria.Nestoridi@esa.int

ESA/ESTEC, PO Box 299, 2200 AG Noordwijk, The Netherlands

1 Introduction

During a previous activity (ESA Contract No. 4000108046/12/NL/LvH: “High Specific Energy Lithium Cells for Space Exploration”) [RD1], Democritus University of Thrace (Prime Contractor), Centre for Research & Technology Hellas (Sub-contractor) and European Space Agency developed and patented [RD2] a novel electrochemical Li-ion secondary cell that exhibits high energy density (>200 Wh/kg) and operates efficiently at subzero temperatures making it attractive to future space applications, e.g. future Landers and surface probes or package missions. Laboratory proof-of-concept tests established TRL3 for the innovative cell.

2 Description of the study

The twofold objective of this activity (ESA Contract No. 4000123741/18/NL/CRS) was:

(i) to increase the TRL by manufacturing industrial-like pouch cells and to validate the technology in relevant environment conditions (TRL4) at Airbus DS facility and
(ii) to investigate the industrialization potential of the technology by performing a market and cost assessment.

DUTH was the Prime Contractor, and **CERTH** and **AIRBUS DS** served as Sub-Contractors. The work was organized into four (4) technical Work Packages (WPs):

WP 1	Technological benchmarking [RD3]
WP 2	New materials development [RD4], [RD5]
WP 3	New technology cell testing [RD6]-[RD7]
WP 4	Market survey and Cost analysis [RD8]-[RD9]

3 WP 1. Technological benchmarking

The aim of this WP was to evaluate two pouch cell manufacturers, Supplier-A and Supplier-B, and finally select one manufacturer for the subsequent campaigns of this Activity. For the manufacturing of the benchmarking cells, DUTH has prepared the Si based anode electrode by sputtering technique, CERTH prepared the electrolyte and then they have been delivered for pouch cell fabrication. The pouch cell fabrication has been carried out by the two suppliers and each supplier have used their own NCA material as a cathode.

Five (5) cells were manufactured Supplier-A and four (4) cells were manufactured by Supplier-B, with a nominal capacity of 1000 mAh (maximum voltage 4.1 V, minimum voltage 2.8 V). The cells have then been submitted to the tests summarized in **Figure 1**.

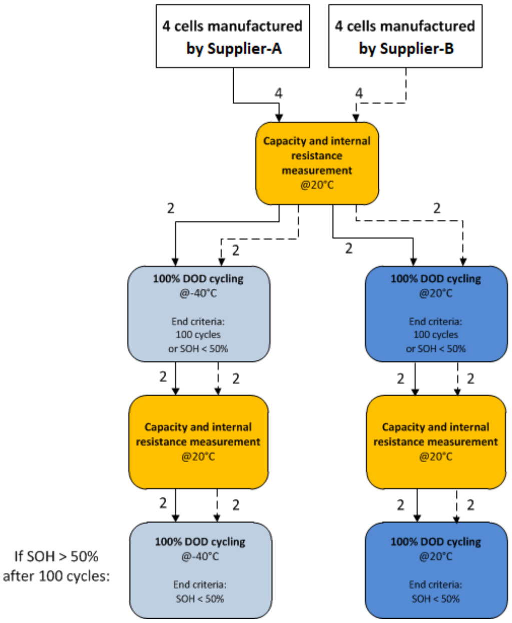

Figure 1: Test flowchart for benchmarking test campaign.

The initial capacity and internal resistance measurements showed that Supplier-A cells have higher initial capacity (Supplier-A: 1076 mAh, Supplier-B: 915 mAh) and energy density (Supplier-A: 158 Wh/kg, Supplier-B: 126 Wh/kg) than Supplier-B cells while they also have much lower initial impedance (Supplier-A: 20.0 mOhm, Supplier-B: 151.6 mOhm) than Supplier-B cells.

The main test aims at measuring the evolution of cell performance during continuous cycling at 100% DOD, under 20°C and -40°C. The test consists of successive 100% DOD cycles. For each cell, the test is stopped when capacity has decreased by 50% relatively to initially measured capacity at the same temperature. This state is defined as End of Life (EoL). Once a cell reaches EoL, it is submitted to a capacity and internal resistance measurement at 20°C again. Cells which perform more than 100 cycles are also submitted to a capacity and internal measurement at 20°C when they reach 100 cycles. The capacity degradation during cycling of each cell at 20°C is depicted in **Figure 2**.

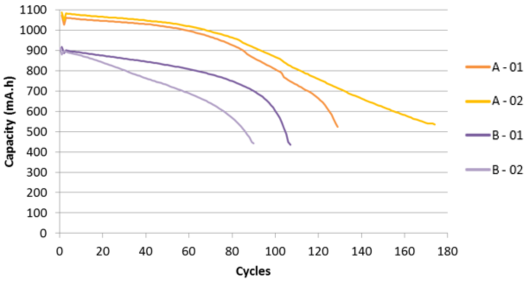

Figure 2: Capacity degradation of benchmarking pouch cells during 100% DOD cycling at 20°C.

It is evident that, Supplier-B cells degrade faster than Supplier-A cells, and one Supplier-B cell has reached EoL at 90 cycles. The other Supplier-B cell demonstrates capacity retention of 61% (at 102 cycles). Supplier-A cells exhibit capacity retention of 86-88 % (at 82 cycles). Furthermore, Supplier-A cells are more consistent in their cycling behaviour than Supplier-B cells at this temperature.

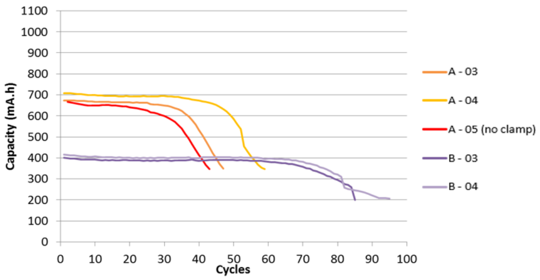

Figure 3: Capacity degradation of benchmarking pouch cells during 100% DOD cycling at -40°C.

Following, the cells were subjected to cycling at -40°C (**Figure 3**). Supplier-A cells are degrading faster than Supplier-B cells, and one Supplier-A cell reached EoL at 48 cycles. The other Supplier-A cell demonstrates capacity retention of 76% (at 53 cycles). Supplier-B cells demonstrate capacity retention of 72-74% (at 82 cycles).

The results of the benchmarking tests campaign can be summarized in the following table:

Criteria	Study target	Supplier-A cells	Supplier-B cells
Capacity at C/10 (mAh)	1000	1076	915
1st cycle coulombic efficiency (%)	>80	~80.5	~75.5
Energy density at 20°C (Wh/kg)	180	158	126
Energy density at -40°C (Wh/kg)	126	97	52
Cycle life at 20°C*	50	110	89 to 105
Cycle life at -40°C*	70	47 to 60	95

* number of cycles before 50% capacity loss

Apart from the stable behavior of Supplier-B cells at -40°C, the Supplier-A cells outperform Supplier-B cells in all criteria. Furthermore, the fact that Supplier-B cells could not deliver the initial capacity of the requested 1000 mAh, was a major pitfall. Based on these results, Supplier-A was selected as the pouch cell manufacturer for the next campaigns of this Activity.

4 WP2. New materials development

The scope of this WP was: (i) to further investigate the electrolyte formulations in order to achieve better performance at the low temperature range operation, and (ii) to test the high deposition rate (HDR) silicon anodes so as to obtain a high energy density anode with a more production-oriented process. Testing was performed in Swagelok® cells. The various Si-based anodes have been prepared and supplied by Fraunhofer FEP (Dresden, Germany) to DUTH for the Swagelok cell fabrication. The low-temperature electrolytes were formulated by CERTH, and the NCA electrode with different mass loadings was supplied by Supplier-A to DUTH.

4.1 Low temperature electrolyte development

For the development of low temperature electrolyte, three components of the electrolyte composition have been investigated: (i) base electrolyte (solvent), (ii) lithium salt, and (iii) ester co-solvent additive, following the development plan shown in **Figure 4**.

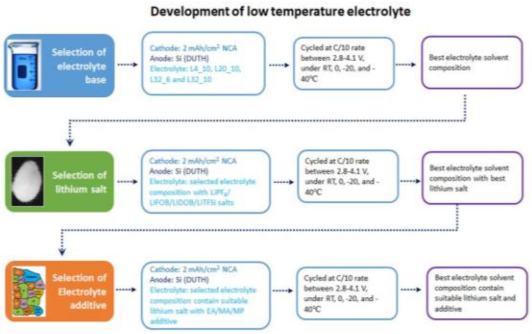

Figure 4: Flowchart for development of high deposition rate anodes.

All Swagelok full-cells contained the NCA cathode (2 mAh/cm^2) from Supplier-A and sputtered Si anode from DUTH. The cells were cycled at C/10 rate under 20°C, 0°C, -20°C and -40°C temperature zones. In order to fix the base solvent composition of electrolyte formulation, four types of electrolyte formulations were prepared based on blends of ethylene carbonate (EC), dimethyl carbonate (DMC), diethyl carbonate (DEC), ethyl methyl carbonate (EMC), ethyl acetate (EA) and fluorinated ethyl carbonate (FEC) and 1 M $LiPF_6$ salt. Cycling data revealed that the addition of EA ester co-solvent as an additive is beneficial for low-temperature operation as it can enhance the physical properties of carbonate-based electrolytes due to their low freezing points, the high ionic conductivity of the resulting electrolytes and low viscosity. Moreover, FEC additive is included in the electrolytes as it is known for stable solid electrolyte (SEI) formation, better lithium-ion reversibility. Therefore, the electrolyte L32, a mixture of EC/DMC/DEC with EA and FEC, was chosen as the base solvent for the following studies.

Once the solvent base of the low-temperature electrolyte was fixed, the research was oriented towards the selection of lithium salts, which can enhance the performance of lithium batteries at low temperature. In addition to the existing $LiPF_6$ salt, three different lithium salts were introduced to the base electrolyte: LiTFSi, LiDOB, and LiFOB. From the cycling data derived from different temperatures, at room temperature and 0°C, all the electrolytes compositions are delivering capacities in a close-range distribution (**Figure 5**). However, at -20 °C and -40°C the L32 electrolyte with 1 M $LiPF_6$ salt is delivering the discharge capacities of 100 and 75 mAh/g, respectively which is higher than 1 M LiTFSi, LiFOB, LiBOB salts containing electrolytes. Therefore, the $LiPF_6$ containing electrolyte composition was chosen for further development as it had delivered better discharge capacities at low temperatures.

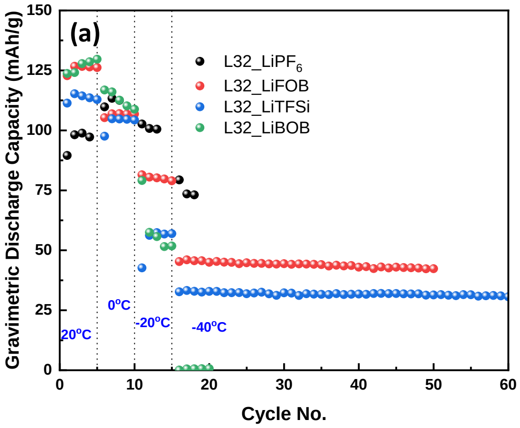

Figure 5: Specific gravimetric discharge capacity of full cells (Si/NCA) containing base electrolyte with different lithium salts at various temperatures.

Finally, in order to enhance the low-temperature operability of lithium batteries, we have investigated two more ester co-solvents as an additive in the base electrolyte instead of EA additive: methyl acetate (MA) and methyl propionate (MP). From the cycling data attained at different temperatures (**Figure 6**), it is observed that the change of ester co-solvents is helpful in terms of increasing capacity. At room temperature, 0°C, and -20°C, the MA and MP additive added electrolytes are performing better than EA additive added electrolyte. However, at -40°C, all the additives are exhibiting similar discharge capacity behaviors at around 75 mAh/g. However, the MP and MA additive added electrolytes had lost a significant amount of discharge capacity when bouncing from -40°C to 20°C and again from 20°C to -40°C, which is undesirable thermal capability behavior. Therefore, it was suggested that EA co-solvent can be a better additive for low-temperature applications.

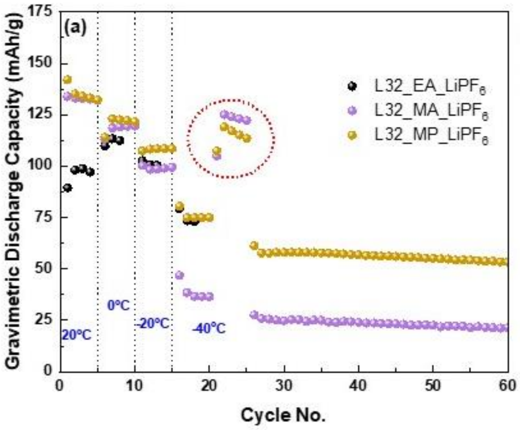

Figure 6: Specific gravimetric discharge capacity of full cells (Si/NCA) containing base electrolyte with different co-solvent ester additives at various temperature conditions.

4.2 Development of higher deposition rate anode

The high deposition rate Si anodes were fabricated and supplied by Fraunhofer FEP. The high deposition rate anodes with different Si mass loadings, ranging between 0.75 and 1.5 mg/cm^2, on copper foil substrates are derived from various coating machines such as Novoflex, Labflex, and Coflex. The Swagelok half cells, composed of developed Si anode and pure lithium metal couple separated by SciMat separator with electrolyte, were cycled at RT with C/10-rate. The electrodes from Novoflex and Coflex are performing better than the electrodes from

Labflex coater (**Figure 7**). The initial capacity loss for the 1.3 mg/cm^2 Si mass loaded electrode produced from Coflex coater is lower than that of the electrodes from Novoflex and Labflex coaters. In terms of stability, both electrodes from Novoflex coater are displaying stable cycling behavior denoting robust mechanical integrity of electrodes. Whereas the 1.3 mg/cm^2 Si mass loaded electrode produced from Coflex coater is slowly losing the capacity over cycling. Based on these results, both Coflex coater derived electrode (1.3 mg/cm^2 Si mass loaded) and Novoflex coater (0.75 mg/cm^2 Si mass loaded) were chosen for the full cell studies.

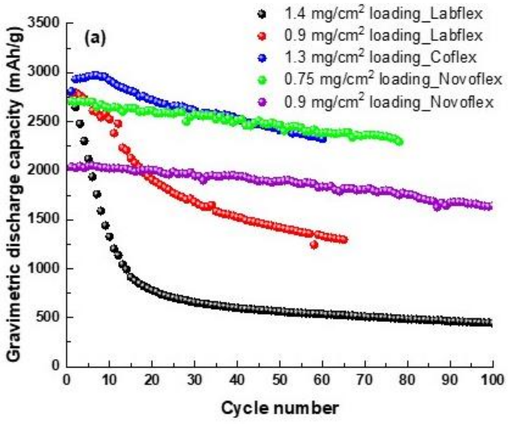

Figure 7: Specific gravimetric discharge capacity of high deposition rate anodes at room temperature.

Full cells were composed of NovoFlex and CoFlex anodes and respective mass loaded NCA cathodes from Supplier-A with L32 base electrolyte containing either EA or MP additives. Full cells were tested again at room temperature, 0^{o}C, -20^{o}C and -40^{o}C (**Figure 8**). Specifically, four (4) potential electrochemical systems were studied:

- **System A1**: Coflex 1/L32 (EA additive)/NCA (3.5 mAh/cm^2)
- **System A2**: Coflex 1/L32 (MP additive)/NCA (3.5 mAh/cm^2)
- **System B1**: Novoflex 1/L32 (EA additive)/ NCA (1.8 mAh/cm^2) and
- **System B2**: Novoflex 1/L32 (MP additive)/ NCA (1.8 mAh/cm^2)

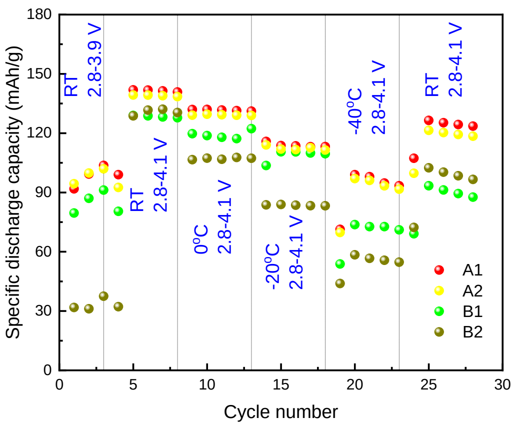

Figure 8: Specific gravimetric discharge capacity of full cells with high deposition rate anodes at room temperature, 0^{o}C, -20^{o}C and -40^{o}C.

The A1 and B1 systems, i.e. EA additive added electrolytes, have exhibited improved behavior than A2 and B2 systems, i.e. MP additive added electrolytes, especially at low temperatures. The A1 system, i.e. EA additive added electrolyte used in higher mass loaded electrode couple had shown higher aerial and specific discharge capacities than other systems. Thus, System A1, comprising of CoFlex coater Si anode (1.3 mg/cm^2), NCA cathode (3.5 mAh/cm^2) from Supplier-A and EA additive added L32 electrolyte, was directed to use in the future campaigns.

5 WP3. New technology cell testing

The objective of WP3 was to implement all features from the development to pouch cells and compare with graphite anode technology. This was realised through two Campaigns.

5.1 First Campaign

The scope of first Campaign was to:

- Compare NCA/Si with NCA/C at low temperature
- Use higher mass loading NCA/Si to increase energy density

For that purpose, two (2) batches of four (4) pouch cells were prepared and characterised at low temperature (-40°C):

- 4 cells with NCA cathode and carbon anode
- 4 cells with NCA cathode and silicon anode

The cells consist in materials which have been developed at Fraunhofer FEP (Si anode), CERTH (low temperature electrolyte) or procured (cathode, separator). The assembly of the cells has been performed by Supplier-A. The nominal capacity of the cells was 1 Ah. The cells. The cells were submitted to a number of tests in Airbus DS laboratory, summarized in **Figure 9**.

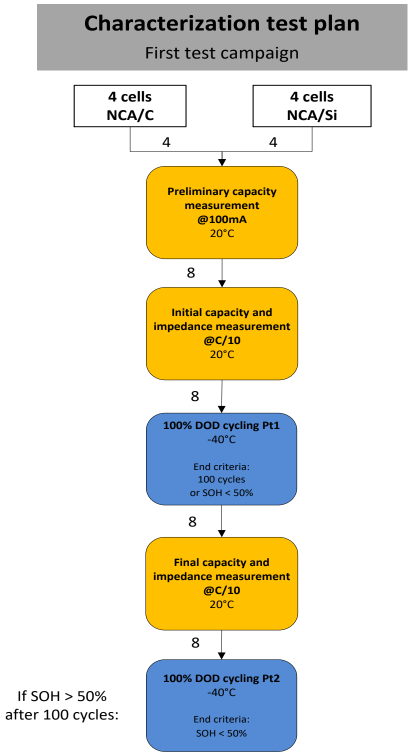

Figure 9: Test flowchart for First test campaign.

Initial capacity and impedance measurements at 20°C showed that NCA/C cells have slightly higher initial capacity and energy density than NCA/Si cells. In addition, the dispersion of capacity and energy of NCA/Si is higher than NCA/C cells. The results are summarized in the following table.

	NCA/C cells	NCA/Si cells
Average capacity	**1104 mAh**	**1028 mAh (-7%)**
Std deviation	**0.7%**	**2.2%**
Average energy density	**189 Wh/kg**	**172 Wh/kg (-9%)**
Std deviation	**0.1%**	**8.9%**

After a first charging at 20°C, the cells' performance was evaluated when cycled at 100% DOD, at -40°C. The capacity of the cells at the beginning of life (BoL) for the two temperatures, 20°C and -40°C, is shown in **Figure 10**.

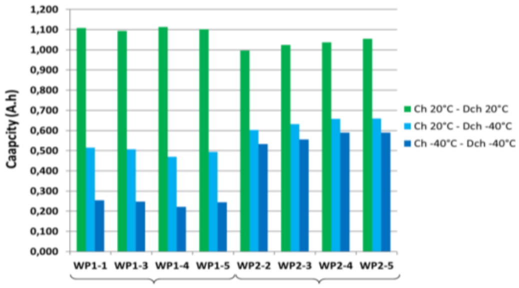

Figure 10: Capacity versus charge and discharge temperature.

When charged and discharged at -40°C, NCA/C cells show a capacity retention of about 23% and an energy density retention of about 19%, compared to their performance at 20°C. On the other hand, NCA/Si cells have much better BoL performance at -40°C, capacity retention of about 55% and an energy density retention of about 52%.

The cycling performance of the cells is demonstrated in **Figure 11**. NCA/C cells have very limited cycle life at -40°C. On the contrary, all NCA/Si cells have much better cycle life at -40°C; however, there is a significant dispersion across the NCA/Si samples. Specifically, the 2 samples with higher mass (denoted as WP2-4 and WP2-5) have a similar performance during cycling at -40°C. They reached EoL at cycle 51 and 57, while the other 2 samples (WP2-2 and WP2-3) started to age more rapidly from cycle 20 and reached EoL around at cycle 34 and 37.

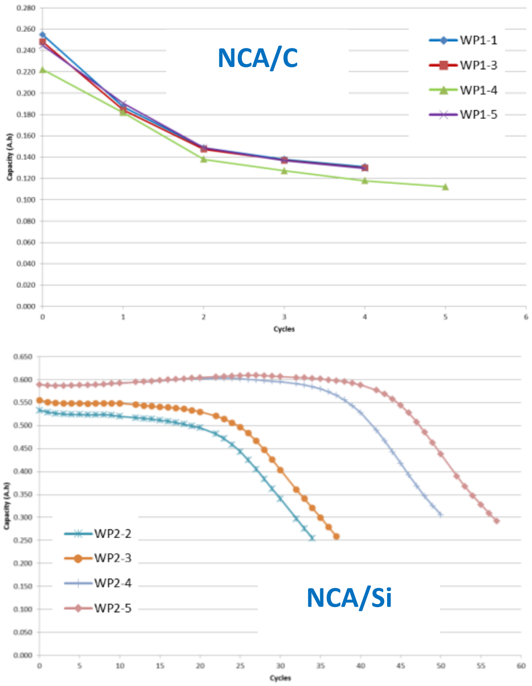

Figure 11: Capacity degradation during 100% DOD cycling at -40°C for NCA/C (top) and NCA/Si (bottom) pouch cells.

The main conclusion from the first Campaign are the following:

- It was clearly demonstrated that the NCA/C system cannot efficiently operate at -40°C as: i) it delivers less than 25% of its nominal capacity, and ii) can only cycle 6 cycles before losing 50% of the initial capacity.
- NCA/Si cells were successfully manufactured by using new Si anodes and they delivered between 187 Wh/kg (for 1 Ah pouch cell at C/10 rate) at 20°C.
- Despite the high electrode mass loading (areal capacity of 3.5 mAh/cm^2), the cells were able to perform at low temperature exhibiting ca. 55% of capacity retention at -40°C. Two of the NCA/Si samples were able to perform 51 and 57 cycles at -40°C before losing 50% of initial capacity, although these samples had lowest initial energy density (156-159 W.h/kg at 20°C). The two samples with the highest energy density (187 W.h/kg) performed 34 and 37 cycles at -40°C.

5.2 Final Campaign

For the Final Campaign twenty (20) pouch cells were fabricated and extensive tests at different charging-discharging profiles were carried out, the purpose being to investigate the compatibility of new cells to Space applications. The deep-drawn pouch cells, composed of silicon anode (Fraunhofer), low temperature electrolyte (CERTH), NCA cathodes (Supplier-A) were assembled by Supplier-A and tested at AIRBUS laboratories. The test plan is summarised in **Figure 12**.

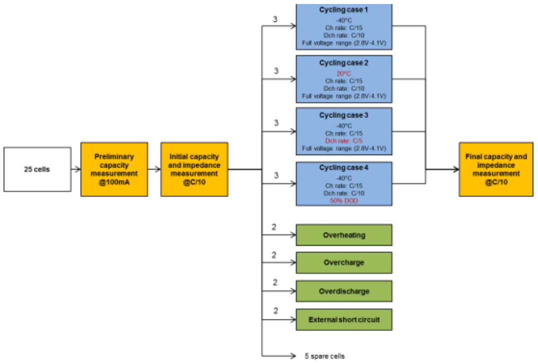

Figure 12: Final Campaign test plan.

5.2.1 Initial characterisation tests

The initial characterization test results at 20°C showed that most samples are performing according to the specifications with a capacity above or close to 1.2 Ah (**Figure 13**). All samples have a coulombic efficiency above or very close to 98% and an energy density between 160 Wh/kg and 170 Wh/kg. Only two cells were excluded from the following testing because of not being able to complete first charge or significantly lower capacity compared to other samples.

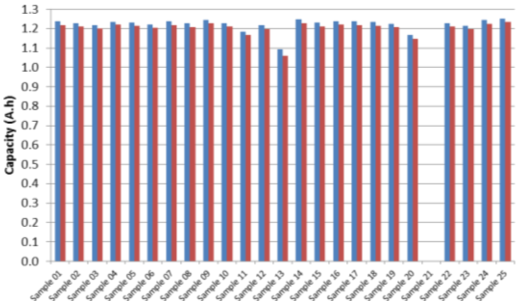

Figure 13: Initial discharge capacity at 20°C.

5.2.2 Cycling tests

Nine (9) of the 12 cells submitted to cycling tests are tested at -40°C. The capacity and impedance measurements performed on these samples at beginning of cycle life at -40°C can be used to characterize the impact of temperature on BoL performance. It was estimated that the average capacity at 20°C was 1216 mAh while at -40°C it dropped to 543 mAh, i.e. -55% relative difference in capacity vs. 20°C. The corresponding gravimetric energy density was 165 Wh/kg and 69 Wh/kg, at 20ºC and -40ºC, respectively (relative difference -58%).

Regarding cycle life to 50% capacity loss, four different cycling cases were investigated:

Cycling case 1: -40°C, Ch rate: C/15, Dch rate: C/10, Full voltage range (2.8V-4.1V)

Cycling case 2: 20°C, Ch rate: C/15, Dch rate: C/10, Full voltage range (2.8V-4.1V)

Cycling case 3: -40°C, Ch rate: C/15, Dch rate: C/5, Full voltage range (2.8V-4.1V)

Cycling case 4: -40°C, Ch rate: C/15, Dch rate: C/10, 50% DOD

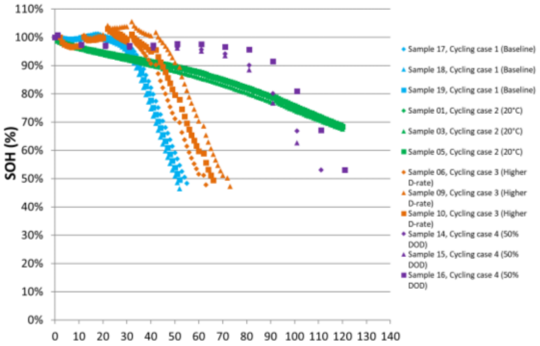

Figure 14: Relative capacity (State of Health) versus cycle life for all cases studied.

The comparison for all cases studies is summarized in **Figure 14**, in terms of relative capacity (State of Health) versus cycle life.

The comparison between cases 1 and 2 depicted the **effect of temperature**. At -40°C, capacity slightly increases and remains stable for approximately 30 cycles, then decreases to 50% loss with a linear trend. At 20°C, the degradation trend is close to linear from the beginning. A slight acceleration of capacity loss can be noticed from cycle 60. These observations were complemented by impedance measurements which showed a decrease during cycle life, and a slight increase before EoL, especially near the end of discharge at -40ºC. At 20°C, impedance is mostly stable (slight increase) at low DOD for the first 80 cycles. The impedance increase is more significant at high DOD.

The **impact of discharge rate** is depicted by comparing cases 1 and 3. The initial capacity loss due to increased discharge rate from C/10 to C/5 is approximately 27%. In both cases, capacity slightly increases and remains stable for approximately 30-40 cycles, then decreases to 50% loss with a linear trend. Cycle life appears to be longer at higher discharge rate. This could be partly because for the same number of cycles performed, the duration of the test is shorter for the C/5 discharge rate case, so the calendar ageing contribution may be smaller. This could also be attributed to the fact that, due to the increased voltage drop caused by impedance, the end of discharge (2.8V) is triggered at a higher state of charge at C/5, compared to the C/10 case. The high discharge rate might have prevented the cells from discharging down to very low state of charge, which is a typical accelerator of ageing.

Finally, the **impact of depth of discharge** was investigated through cases 1 and 4. The cycle life to 50% capacity loss for case 1 (baseline, full voltage range) was 52-55 cycles while for case 4 (50% DOD) it was 110-124 cycles. For both cases, impedance decreases progressively during cycle life, and increases slightly before EoL, especially near the end of discharge.

After cycling the cells were conducted a final capacity check (**Figure 15**). Compared to their initial state at 20°C, samples cycled at -40°C have lost between 32% and 55% of capacity. The 3 samples submitted to cycling case 3 (-40ºC, C/5 discharge rate), have significantly more end of life capacity at 20°C, compared to the other cells cycled at -40°C (case 1 and 4). This is mainly due to the fact that the 50% capacity loss triggering EoL was calculated from C/5 discharges for case 3, whereas it was calculated from C/10 discharges for cases 1 and 4.

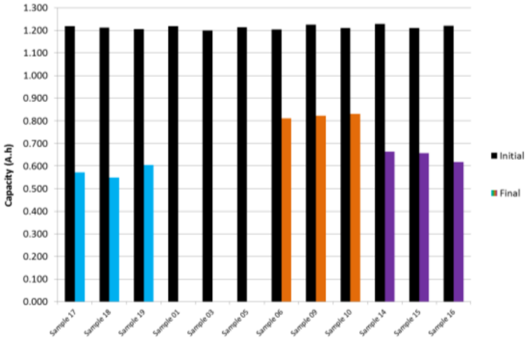

Figure 15: Initial and final capacity of each sample at 20°C.

5.2.3 Abusive tests

A number of abusive/safety tests were performed in the pouch cells, including: (i) overheating, (ii) overcharge, (iii) overdischarge, and (iv) external short circuit.

The behaviours of the 2 tested samples were significantly different for the **overheating** test. One sample exhibited thermal runaway with explosion and flame release triggered at 280°C, accompanied by a slight voltage decrease during the last few minutes before thermal runaway and a voltage drop to 0V at the moment of explosion. The second sample had a thermal runaway without explosion and flame release triggered at 478°C. Its voltage decreases to approximately 3V when temperature increases from 200°C and 300°C, then erratic variation of voltage between 0V and 3V until thermal runaway is triggered.

Overcharging was performed in two steps, one with charge current of 100 mA for 80h followed by 1A for 1h. During step 1 (100 mA), voltage increase to 5.11V and stay at this value approximately 24h. After, it steps up at 6.06V, then decreased at 5.69 V until the end of 80h. During step 2, there is no thermal runaway, consequently, current limit is fixed to 1A and limit voltage at 32 V during 1 hour. The voltage does not increase more than 12V and temperatures continue to raise during this step. After charging at 1 A for 19 min 54 sec, there is a short circuit on the cell.

The scope of the **overdischarge** test is the evaluation of cell behavior when discharged below recommended minimum voltage. Cells were overdischarged at 20°C by constant current (CC) discharge @100mA, to 0V or until cell failure. If voltage reaches 0V, constant-voltage discharge at 0V for 1h or until cell failure. A similar behavior was observed for the 2 samples. No physical damage or significant heating observed during discharge to 0V, or during constant-voltage discharge at 0V during 1h. Voltage decrease to 0V: quick drop of voltage between 2.5V and 1V, and at the very end between 0.75V and 0V.

Before the **external short circuit** test, cells were fully charged (C/10 to 4.1V, then CV charge to C/100) at 20°C. For both samples, the maximum short-circuit current is approximately 250A and it is reached in less than 100µs. After maximum current is reached, discharge current decreases back to 10A (i.e. 10C) in 129s or 169s depending on the sample. No physical damage observed during the test and after the test, no weight loss, while no apparent release of gas or tearing of pouch.

5.3 Market survey

A market survey on industrial solutions for the development of Si-based anodes using a Roll-to-Roll DC sputtering system in a pilot manufacturing line has been conducted. After defining the required specifications of the equipment, based on the specifications of the materials that have been used and developed so far, several industrial equipment manufacturers from both the European and the North American market have been examined.

Available equipment includes small-scale Roll-to-Roll Physical Vapor Deposition (PVD) systems that are suitable for pilot manufacturing lines and can be modified for DC magnetron sputtering of Silicon targets on 300mm-wide metal foils. Web meetings with suppliers of such equipment have been held in order to discuss about the requirements of our application and acquire information on their proposed systems along with respective technical details such as footprint, throughput, yield, downtime/uptime ratio, delivered and commissioned cost, operational cost, etc.

Most Roll-to-Roll deposition systems are custom designs to meet the specific requirements of each application. Thus, different options have been examined, such as the possibility of using the maximum available metal foil width that can be provided by the supplier and designing a system that can offer simultaneous double-sided deposition, in an effort to optimize the system throughput.

5.4 Cost analysis

Based on the technical requirement of the new NCA/Si cell and all data acquired through the previous Task, cost estimations have been conducted for different scenarios. Required materials, such as Silicon Anodes, NCA Cathodes, Electrolyte solutions and Pouch cells could be either outsourced or developed in-house. Moreover, cost estimations include CAPEX depreciation over a 10-year period for the required industrial equipment of Roll-to-Roll sputtering that was investigated in the previous Task. Finally, the impact of the metal foil dimensions on the total cost per Ah of capacity has been evaluated. The results and estimations of this report provide the groundwork for the production of the NCA/Si cells in a small-scale pilot manufacturing line.

6 Conclusions

During this activity, we were able to evaluate our electrochemical system with respect to: (i) silicon anode fabricated at an industrial scale equipment, (ii) pouch cells that were manufactured at different suppliers and tested by Airbus Defense and Space and (iii) safety protocols. In addition, we showed that the standard graphitic-based chemistry cannot operate at low temperatures. Finally, we evaluated the Cost of Ownership of our products.

Our innovative pouch cells exhibit around 185 Wh/kg (total cell mass) of energy density and can be efficiently charged and discharged at -40°C with a capacity retention of around 50% (**Figure 16**). For the Martian rover application, the number of cycles attained when the cell was charged and discharged at -40°C is on average 117 (Depth of Discharge:50%, C/15, D/10) and 68 (Depth of Discharge:100%, C/15, D/5). The activity has proven that this innovative technology largely beat the standard technology at the low temperature range and can be applied to the Martian Rover application. Moreover, it has been demonstrated the technology is safe and can be industrialized.

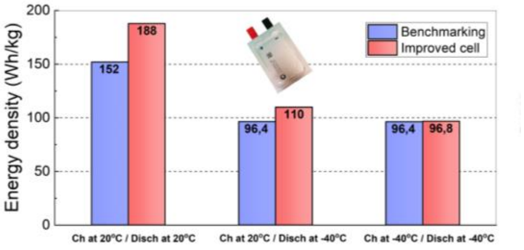

Figure 16: Comparison of low temperature performance of the HELT-Bat with benchmarking cells.

The future plan of the activity is to further improve the characteristics and the performance of the product and to decrease the Cost of Ownership in order to adapt it to space and terrestrial applications. Funding through a GSTP programme is one of the main targets of this activity.

7 References

[RD1] Final Report, "High Specific Energy Lithium Cells for Space Exploration" (ESA Contract No. 4000108046/12/NL/LvH)
[RD2} "Rechargeable Electrochemical Lithium Ion Cell", US 2019/0260084 A1 (2019).
[RD3] Results of benchmarking cells (D1)
[RD4] Characterization test plan, (D2)
[RD5] Characterization report (D3)
[RD6] First campaign test report (D4)
[RD7] Final campaign test report (D5)
[RD8] Market survey on industrial equipment (D6)
[RD9] Cost analysis report (D7)